RSC Advances

RSC Advances

www.rsc.org/advances

ROYAL SOCIETY OF CHEMISTRY

www.rsc.org/advances

Journal Name

Dynamic Article Links ▶

ARTICLE TYPE

Synthesis of Ag nanoparticles-carbon nanotube-reduced graphene oxide hybrids for highly sensitive non-enzymatic hydrogen peroxide detection†

Yong Zhang,[a,b] Ziying Wang,[a] Ye Ji,[a] Sen Liu*[a] and Tong Zhang*[a,b]

Ag nanoparticles-carbon nanotube-reduced graphene oxide (AgNPs-CNT-rGO) hybrids have been synthesized by reduction of GO in CNT-GO hybrids and AgNO₃. The linear detection range and detection limit of the H₂O₂ sensor based on AgNPs-CNT-rGO hybrids were estimated to be from 0.01 mM to 10 mM (R=0.997), and 1 µM, respectively.

Introduction

Nowadays, the determination of hydrogen peroxide (H_2O_2) is becoming increasingly important. H_2O_2 play a significant role in industry, such as oxidant in the chemical industry, bleaching agent in textile printing and dyeing industry, and disinfectant in pharmaceutical industry. Furthermore, H_2O_2 is not only a by-product of several highly selective oxidases, but also an essential mediator in food, clinical and environmental analyses.[1-3] Therefore, it is worthwhile to develop a rapid, simple, accurate and reliable method for determination of H_2O_2. Particularly, the electrochemical technique has been well accepted as a promising technique for H_2O_2 detection due to its excellent advantages such as cost-effectiveness, fast response, good stability, high sensitivity and selectivity.[4-6]

For electrochemical detection of H_2O_2, Ag nanoparticle (AgNP) is one of the most effective materials because of its excellent catalytic activity toward electrochemical reduction of H_2O_2.[7] In order to further enhance the performances of AgNP, the reduced graphene oxide (rGO) has been used to fabricate AgNPs-rGO nanocomposites for fabrication of highly effective H_2O_2 sensors.[8,9] The popularity of graphene is due to the fact that its honeycomb lattice molecular structure leads to remarkable physical and chemical properties, such as high surface area, high thermal and electrical conductivity, high chemical stability.[10-13] Indeed, AgNPs-rGO hybrids exhibit better sensing performances than the AgNPs in the absence of rGO owing to the outstanding synergetic properties of noble metal NPs and rGO. However, previous researches have shown that the performances of rGO-based supports are obviously depressed by the restacking phenomenon of rGO reduced from GO.[14,15] The rGO tends to form an irreversible aggregation because of the intensive π-π interaction among the rGO layers during the chemical reaction process, which also obstructs the uniformity of materials and subsequent the performance of electrochemical sensor. Therefore,

the technology to overcome the restacking of rGO should be pursued for applications related to electrochemical sensors.

It is well-know that carbon nanotube (CNT) is also an attractive choice of carbon matrix, which is one-dimensional nanomaterial consisted of one or multiple cylinders of carbon sheets.[16,17] Some researchers have reported that CNT can be well-dispersed in GO aqueous solution after ultrasonication and absorbed onto the GO surface through π-π attraction.[18,19] By using this method, the CNT-GO composites can be obtained and then the reduction of CNT-GO could fabricate the CNT-rGO composites. The assembly rGO with CNT effectively increases the electric conductivity and hinders restacking of rGO layers, inducing facile transfer of electrons from CNT and reactants through the interspace of rGO layers.[14,20] Hence, the CNT-rGO composites provide a new route to overcome the restacking of rGO and the assembly rGO with CNT provides a promising method to prepare high-performance rGO-based composites for electrochemical sensing applications.[21] It is worth mentioning that numerous CNT-rGO-based composites have been successfully synthesized and applied in various fields, such as supercapacitors,[22] capacitive deionization,[23] cathode catalyst for oxygen reduction reaction,[24] and so on.

In this paper, the reduction of GO in mixture of CNT-GO and AgNO₃ aqueous solution has been developed to construct AgNPs-CNT-rGO hybrids. The CNT-GO composites can be prepared by self-assembly process that CNT could be dispersed into GO aqueous solution after sonication. The application of AgNPs-CNT-rGO hybrids has been demonstrated for electrochemical detection of H_2O_2, leading to a high-performance non-enzymatic H_2O_2 sensor. Moreover, the AgNPs-CNT-rGO hybrids have also been proven to be effective for selective determination of H_2O_2.

Results and discussion

The synthetic route for the AgNPs-CNT-rGO hybrids is shown in Scheme 1. In the present work, GO was obtained via the modified Hummers' method and used to fabricate CNT-GO composites. It is well known that the CNT could be well-dispersed in GO aqueous solution and absorbed onto the GO surface through π-π attractions.[18,19] Finally, the AgNPs-CNT-rGO hybrids were constructed by the reduction process, where GO in CNT-GO composites and Ag⁺ aqueous solution were reduced in the

presence of NaOH at 80 ºC under stirring.
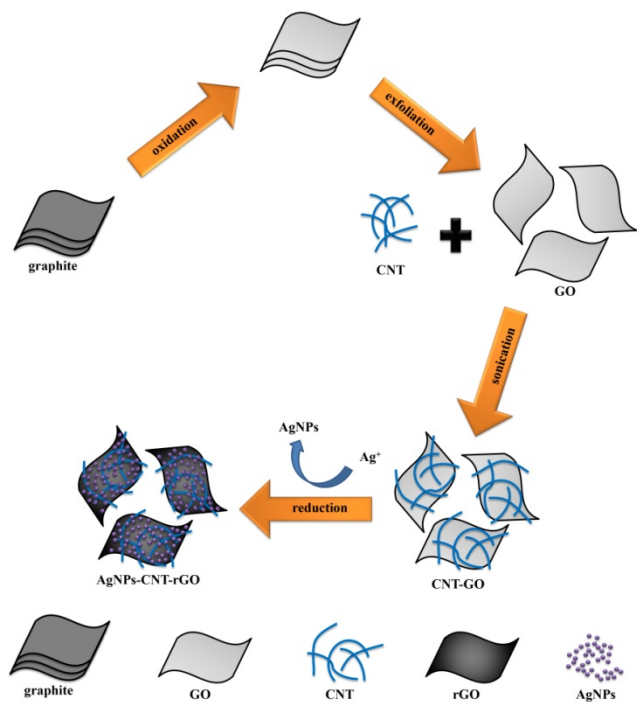
Scheme 1 Schematic illustration of the fabrication and architecture of AgNPs-CNT-rGO hybrids.

Fig. 1a shows the Raman spectra of GO, CNT-GO and AgNPs-CNT-rGO hybrids, revealing a D band at about 1339 cm^{-1} and a G band at about 1591 cm^{-1}, which are attributed to the breathing mode of k-point phonons of A_{1g} symmetry and the first-order scattering of the E_{2g} phonons, respectively.[25] According to the previous reports,[26-28] the intensity of D band to G band increased, when GO was reduced to form rGO. In this work, the intensity of D band to G band for AgNPs-CNT-rGO hybrids (1.14) is larger than that of CNT-GO (1.02) and GO (1.06), indicating the formation of new graphitic domains after the reduction of CNT-GO. This result confirms the formation of rGO by reduction of GO during the synthesis process for AgNPs-CNT-rGO hybrids.
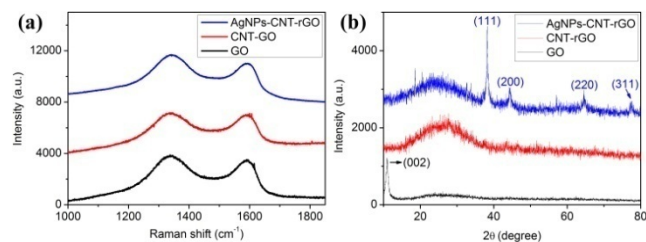
Fig. 1 (a) Raman spectra of GO (black line), CNT-GO (red line) and AgNPs-CNT-rGO (blue line); (b) XRD patterns of GO (black line), CNT-rGO (red line) and AgNPs-CNT-rGO (blue line).

Fig. 1b shows the X-ray diffraction (XRD) patterns of GO, CNT-rGO composites and AgNPs-CNT-rGO hybrids, respectively. It is seen that GO exhibits a strong diffraction peak at 2θ of 11.06° attributed to (002) diffraction of GO, indicating the formation of GO by Hummers' method from graphite powder.

Note that this peak disappears in the XRD patterns of CNT-rGO composites and AgNPs-CNT-rGO hybrids, indicating the reduction of GO into rGO in the presence of NaOH at 80 ºC. Furthermore, compared to XRD pattern of CNT-rGO, four diffraction peaks at 2θ of 38.22°, 44.38°, 64.52° and 77.48° are observed for AgNPs-CNT-rGO hybrids, which are indexed as (111), (200), (220) and (311) diffractions of a face-centered cubic crystal of Ag.[29] These observations indicate the successful preparation of AgNPs-CNT-rGO hybrids.
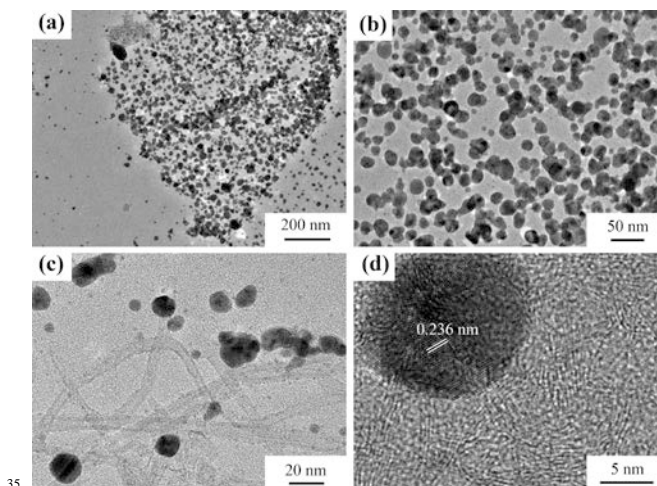
Fig. 2 (a)-(d) TEM images of the obtained AgNPs-CNT-rGO hybrids.

Fig. 2a shows typical transmission electron microscope (TEM) images of AgNPs-CNT-rGO hybrids. A large amount of NPs with diameters of a few nanometers to several tens of nanometers are observed. As shown in Fig. 2b, there is no large block of Ag in AgNPs-CNT-rGO hybrids, although no surfactant was used in the process of material preparation. Furthermore, the aggregation of AgNPs did not happen in AgNPs-CNT-rGO hybrids. These results can be attributed to the nucleation and growth of AgNPs on the surface of CNT-GO in the preparation process of AgNPs-CNT-rGO hybrids, indicating that the CNT-rGO composites are good supporting materials to load AgNPs. There are some CNT on the rGO sheet, indicating the formation of CNT-rGO composites in the final samples, as shown in Fig. 2c. Fig. 2d shows high resolution TEM image of AgNPs-CNT-rGO hybrids. It is seen that one nanoparticle exhibits clear lattice fringes with an interplane distance of 0.236 nm corresponding to the (111) lattice space of Ag, providing a piece of evidence to support that the NPs are AgNPs. All results support the synthesis of AgNPs-CNT-rGO hybrids and indicate that the CNT-rGO composites are good supporting materials to load AgNPs.

The content of the AgNPs in AgNPs-CNT-rGO hybrids was characterized by thermogravimetric analysis (TGA) curve, as shown in Fig. 3. The weight loss from room temperature to 250 ºC is 11.42%, which is attributed to desorption of surface bound water and other gas molecules. The weight loss from 250 ºC to 550 ºC is about 40.73%, attributed to the removal of oxygen-containing groups and the decomposition of carbon framework from the hybrids.[25] The weight loss from 550 ºC to 800 ºC remains constant. The residual weight is about 47.85%, attributed to the content of AgNPs in AgNPs-CNT-rGO hybrids.
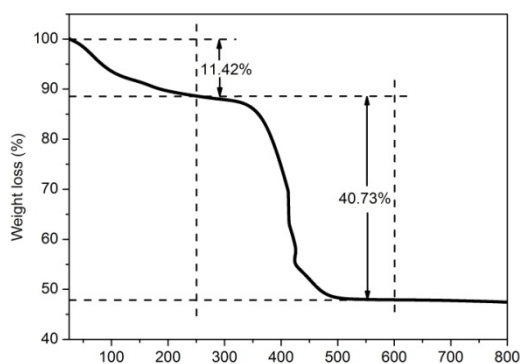
Fig. 3 TGA curve of AgNPs-CNT-rGO hybrids.

Electrochemical H_2O_2 sensor was constructed to demonstrate the sensing performance of AgNPs-CNT-rGO hybrids. Fig. 4a
5 shows cyclic voltammograms (CVs) of a bare glassy carbon electrode (GCE), AgNPs-rGO/GCE and AgNPs-CNT-rGO/GCE in the presence of 1 mM H_2O_2, and AgNPs-CNT-rGO/GCE in the absence of H_2O_2 in N_2-saturated 0.2 M phosphate buff saline (PBS) at pH 6.5. It can be clearly seen that the response of the
10 bare GCE to H_2O_2 is pretty weak. In contrast, the AgNPs-CNT-rGO/GCE exhibits a remarkable catalytic current peak about 33.5 μA at -0.38 V in the presence of 1 mM H_2O_2 and no obvious reduction current is observed for AgNPs-CNT-rGO/GCE in the absence of H_2O_2. These results indicate that AgNPs-CNT-rGO
15 can catalyze reduction of H_2O_2. As shown in Fig. S1, the current peak of AgNPs/GCE is 26.1 μA at -0.56 V in the presence of 1 mM H_2O_2, which is lower than that of AgNPs-CNT-rGO, indicating that the CNT-rGO composites as good supporting materials can improve the catalytic activity of AgNPs. The
20 catalytic current peak of AgNPs-rGO/GCE is 31.7 μA at -0.51 V in the presence of 1 mM H_2O_2. The both current peak and potential of AgNPs-CNT-rGO/GCE are higher than those of AgNPs-rGO/GCE, indicating the enhancing the sensing performances of rGO-AgNPs hybrids by introduction of CNT.
25 Hence, AgNPs-CNT-rGO hybrids could be used as a promising material for fabrication of non-enzymatic H_2O_2 sensor.

The effect of pH value of PBS buffer solution on the AgNPs-CNT-rGO/GCE was examined, as shown in Fig. S2. The AgNPs-CNT-rGO/GCE shows different responses with the pH of 0.2 M
30 PBS buffer solution from 6.0 to 7.5 in the presence of 1 mM H_2O_2. It is seen that the current attributed to the reduction of H_2O_2 increases with increasing pH value from 6.0 to 6.5 and reaches a maximum at pH value of 6.5. Then, the current decreases as pH was further increased. Therefore, the PBS buffer
35 solution at pH 6.5 is selected as the supporting electrolyte in this work, and this result is same as the previous reports.[5,30]

Furthermore, the effect of scan rate on sensing performances of AgNPs-CNT-rGO/GCE for detection of H_2O_2 was also examined, as shown in Fig. S3. It is seen that the peak current increases
40 accordingly with the scan rates in the range of 10~150 mV s^{-1}. The peak currents increase linearly with the square root of scan rate, indicating the diffusion-controlled processes for detection of H_2O_2.[26]

Fig. 4b shows the typical current-time plots of AgNPs-CNT-
45 rGO/GCE in 0.2 M PBS buffer solution (pH 6.5) under stirring

on consecutive step change of H_2O_2 concentrations at an applied potential of -0.3 V. The current-time curve of the AgNPs-CNT-rGO/GCE for low concentrations of H_2O_2 is shown in Fig. 4c. When an aliquot of H_2O_2 was dropped into the stirring PBS
50 solution, the reduction current rose steeply to reach a stable value. The AgNPs-CNT-rGO/GCE could accomplish 95% of the steady state current within 2 s, indicated a fast amperometric response behavior. Fig. 4d shows the corresponding calibration curve of AgNPs-CNT-rGO/GCE. The linear detection range was
55 estimated to be from 0.01 to 10 mM (R=0.997). Fig. 4e shows the response of the sensor based on AgNPs-CNT-rGO exposed to 1 μM H_2O_2 in 0.2 M PBS at pH 6.5, indicating that the detection limit of H_2O_2 sensor based on AgNPs-CNT-rGO is 1 μM.

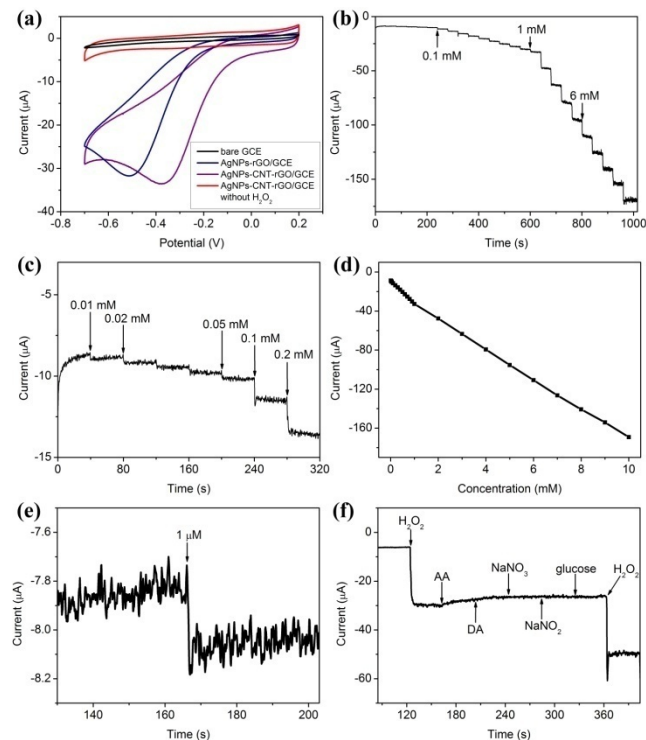60 **Fig. 4** (a) Cyclic voltammograms (CVs) of different electrodes in N_2-saturated 0.2 M PBS at pH 6.5 in the presence and absence of 1 mM H_2O_2 (scan rate: 50 mV s^{-1}); (b) and (c) typical steady-state response of AgNPs-CNT-rGO/GCE to successive injection of H_2O_2 into the stirred 0.2 M PBS at pH 6.5 (applied potential: -0.30 V); (d) the corresponding calibration
65 curve; (e) steady-state response of AgNPs-CNT-rGO/GCE exposed to H_2O_2 (1 μM) in 0.2 M PBS/ pH 6.5; (f) Steady-state response of AgNPs-CNT-rGO/GCE exposed to AA, DA, NaNO₃, NaNO₂ (0.1 mM), glucose and H_2O_2 (1 mM) each.

The influence from common interferences species such as
70 ascorbic acid (AA), dopamine (DA), NaNO₃, NaNO₂ and glucose was also investigated. As shown in Fig. 4f, the amperometric responses of AgNPs-CNT-rGO/GCE is strong by the addition of H_2O_2 (1 mM) in 0.2 M PBS buffer solution (pH 6.5) at a working potential of -0.3 V, and no significant changes to the addition of
75 five relevant electroactive species (AA, DA, NaNO₃, NaNO₂, 0.1 mM and glucose, 1 mM) is observed. These observations indicate the anti-interference advantage of AgNPs-CNT-rGO hybrids. The sensing performance of the H_2O_2 based on AgNPs-CNT-rGO hybrids was compared with the previously reported H_2O_2 sensors
80 based on AgNPs, as shown in Table 1. It is seen that the AgNPs-

CNT-rGO hybrids have wider linear range and lower detection limit. Compared with poly(m-phenylenediamine),[31] attapulgite[32] and rGO,[26,33,34] the CNT-rGO composites are more remarkable as the modified material to improve the performance of AgNPs-based for H_2O_2 detection.

Table 1 Comparison of results from this work and literature regarding performance of H_2O_2 assays.

Electrode material	Performance		Reference
	LOD[a] (μM)	Linear range (mM)	
AgNPs/GCE	2	-	7
AgNPs-PMPD[b]/GCE	4.7	0.1-30	31
AgNPs-ATP[c]/GCE	2.4	0.01-21.53	32
AgNPs-rGO/GCE[e]	1.8	0.1-60	26
AgNPs-rGO/ITO[d]	5	0.1-100	33
AgNPs-rGO/GCE[f]	4.3	0.1-70	34
AgNPs-CNT-rGO/GCE	1	0.01-10	This work

[a] LOD-limit of detection.
[b] PMPD-poly(m-phenylenediamine).
[c] ATP-attapulgite.
[d] ITO-indium tin oxide.
[e] AgNPs-rGO/GCE-The AgNPs-rGO was prepared by the hydrothermal reaction.
[f] AgNPs-rGO/GCE-The AgNPs-rGO was prepared by the ultrasonic reaction.

The stability, reproducibility and repeatability of AgNPs-CNT-rGO/GCE were also examined. It was seen that the AgNPs-CNT-rGO/GCE remained 94% of its initial current response to H_2O_2 after 10 days' storage, indicating the good stability of the H_2O_2 sensor. The reproducibility was estimated from the response to 1 mM H_2O_2 at five modified electrodes prepared in the same conditions and a relative standard deviation (RSD) of 2.7% was obtained. The RSD of the amperometric response to 1 mM H_2O_2 was 3.4% for 5 successive measurements, indicated the good repeatability of AgNPs-CNT-rGO/GCE.

To examine the accuracy and applicability of AgNPs-CNT-rGO/GCE, the real sample analysis was carried out by detection of H_2O_2 in milk sample. The supernatant liquid was obtained from pasteurized milk sample, according to the previous reports.[35,36] Table S1 shows the results of detection of H_2O_2 at AgNPs-CNT-rGO/GCE in milk sample solution. It is seen that the recoveries of H_2O_2 samples with concentrations of 100 and 200 μM are 97.3% and 94.9%, respectively, suggesting the potential application to the detection of H_2O_2 in real samples.

Conclusion

In summary, the AgNPs-CNT-rGO hybrids have been successfully prepared and the AgNPs-CNT-rGO/GCE has been fabricated and demonstrated for a high-performance non-enzymatic detection of H_2O_2. Our present work provides a novel method for development of high performance electrochemical sensors using CNT-rGO-based materials.

Acknowledgments

Notes and references

[a] State Key Laboratory of Integrated Optoelectronics, College of Electronic Science and Engineering, Jilin University, Changchun, P. R. China
[b] State Key Laboratory of Transducer Technology, Chinese Academy of Sciences, P. R. China
*Corresponding authors: E-mail: zhangtong@jlu.edu.cn (T. Zhang); liusen@jlu.edu.cn (S. Liu); Fax: +86 431 85168270; Tel: +86 431 85168385
† Electronic Supplementary Information (ESI) available: Material and methods, CVs of AgNPs-CNT-rGO/GCE in PBS with different pH, CVs of AgNPs-CNT-rGO/GCE at different scan rates. See DOI: 10.1039/b000000x/

1 W. Chen, S. Cai, Q.-Q. Ren, W. Wen and Y.-D. Zhao, *Analyst*, 2012, **137**, 49-58.
2 Y. Hitomi, T. Takeyasu, T. Funabiki and M. Kodera, *Anal. Chem.*, 2011, **83**, 9213-9216.
3 H. Tan, C. Ma, Q. Li, L. Wang, F. Xu, S. Chen and Y. Song, *Analyst*, 2014, **139**, 5516-5522.
4 M. Sawangphruk, Y. Sanguansak, A. Krittayavathananon, S. Luanwuthi, P. Srimuk, S. Nilmoung, S. Maensiri, W. Meevasana and J. Limtrakul, *Carbon*, 2014, **70**, 287-294.
5 A.T. Ezhil Vilian, S.-M. Chen and B.-S. Lou, *Biosens. Bioelectron.*, 2014, **61**, 639-647.
6 Q.-L. Zhang, D.-L. Zhou, Y.-F. Li, A.-J. Wang, S.-F. Qin and J.-J. Feng, *Microchim. Acta*, 2014, **181**, 1239-1247.
7 C. M. Welch, C. E. Banks, A. O. Simm and R. G. Compton, *Anal. Bioanal. Chem.*, 2005, **382**, 12-21.
8 Q. Li, X. Qin, Y. Luo, W. Lu, G. Chang, A. M. Asiri, A. O. Al-Youbi and X. Sun, *Electrochim. Acta*, 2012, **83**, 283-287.
9 S. Liu, L. Wang, J. Tian, Y. Luo, X. Zhang and X. Sun, *J. Colloid Interface Sci.*, 2011, **363**, 615-619.
10 R. Devasenathipathy, V. Mani and S.-M. Chen, *Talanta*, 2014, **124**, 43-51.
11 X. Huang, X. Qi, F. Boey and H. Zhang, *Chem. Soc. Rev.*, 2012, **41**, 666-686.
12 J.-J. Lv, A.-J. Wang, X. Ma, R.-Y. Xiang, J.-R. Chen and J.-J. Feng, *J. Mater. Chem. A*, 2015, **3**, 290-296.
13 L. Wang, X. Lu, C. When, Y. Xie, L. Miao, S. Chen, H. Li, P. Li and Y. Song, *J. Mater. Chem. A*, 2015, **3**, 608-616.
14 Y. Bai, M. Du, J. Chang, J. Sun and L. Gao, *J. Mater. Chem. A*, 2014, **2**, 3834-3840.
15 Y.-S. Wang, S.-Y. Yang, S.-M. Li, H.-W. Tien, S.-T. Hsiao, W.-H. Liao, C.-H. Liu, K.-H. Chang, C.-C.M. Ma and C.-C. Hu, *Electrochim. Acta*, 2013, **87**, 261-269.
16 R. Chen, T. Zhao, J. Lu, F. Wu, L. Li, J. Chen, G. Tan, Y. Ye and K. Amine, *Nano Lett.*, 2013, **13**, 4642-4649.
17 C. Sumathi, P. Muthukumaran, S. Radhakrishnan, J. Wilson and A. Umar, *RSC Adv.*, 2014, **4**, 23050-23057.
18 C. Zhang, L. Ren, X. Wang and T. Liu, *J. Phys. Chem. C*, 2010, **114**, 11435-11440.
19 T. Sun, Z. Zhang, J. Xiao, C. Chen, F. Xiao, S. Wang and Y. Liu, *Sci. Rep.*, 2013, **3**, 2527.
20 C. H. Choi, M. W. Chung, H. C. Kwon, J. H. Chung and S. I. Woo, *Appl. Catal. B Environ.*, 2014, **144**, 760-766.
21 K.-Y. Hwa and B. Subramani, *Biosens. Bioelectron.*, 2014, **62**, 127-133.
22 S.-M. Li, Y.-S. Wang, S.-Y. Yang, C.-H. Liu, K.-H. Chang, H.-W. Tien, N.-T. Wen, C.-C.M. Ma and C.-C. Hu, *J. Power Sources*, 2013, **225**, 347-355.
23 Y. Wimalasiri and L. Zou, *Carbon*, 2013, **59**, 464-471.
24 Z. Jin, H. Nie, Z. Yang, J. Zhang, Z. Liu, X. Xu and S. Huang, *Nanoscale*, 2012, **4**, 6455-6460.
25 S. Liu, B. Yu, H. Zhang, T. Fei and T. Zhang, *Sens. Actuators B*, 2014, **202**, 272-278.
26 X. Qin, Y. Luo, W. Lu, G. Chang, A. M. Asiri, A. O. Al-Youbi and X. Sun, *Electrochim. Acta*, 2012, **79**, 46-51.
27 J. Tian, S. Liu, Y. Zhang, H. Li, L. Wang, Y. Luo, A. M. Asiri, A. O. Al-Youbi and X. Sun, *Inorg. Chem.*, 2012, **51**, 4742-4746.

28 S. Stankovich, D. A. Dikin, R. D. Piner, K. A. Kohlhaas, A. Kleinhammes, Y. Jia, Y. Wu, S. T. Nguyen and R. S. Ruoff, *Carbon*, 2007, **45**, 1558-1565.

29 B. Yu, J. Feng, S. Liu and T. Zhang, *RSC adv.*, 2013, **3**, 14303-14307.

5 30 Y. Tian, F. Wang, Y. Liu, F. Pang and X. Zhang, *Electrochim. Acta*, 2014, **146**, 646-653.

31 J. Tian, H. Li, W. Lu, Y. Luo, L. Wang and X. Sun, *Analyst*, 2011, **136**, 1806-1809.

32 H. Chen, Z. Zhang, D. Cai, S. Zhang, B. Zhang, J. Tang and Z. Wu,
10 *Talanta*, 2011, **86**, 266-270.

33 A. M. Golsheikh, N. M. Huang, H. N. Lim, R. Zakaria and C.-Y. Yin, *Carbon*, 2013, **62**, 405-412.

34 A. M. Golsheikh, N. M. Huang, H. N. Lim and R. Zakaria, *RSC Adv.*, 2014, **4**, 36401-36411.

15 35 J. S. Easow and T. Selvaraju, *Electrochim. Acta*, 2013, **112**, 648-654.

36 L. Zheng, D. Ye, L. Xiong, J. Xu, K. Tao, Z. Zou, D. Huang, X. Kang, S. Yang and J. Xia, *Anal. Chim. Acta*, 2013, **768**, 69-75.